

Eu³⁺ Luminescence, Ce⁴⁺ → Eu³⁺ Energy Transfer, and White-Red Light Generation in Sr₂CeO₄

R. Sankar^a and G. V. Subba Rao^{b,*}

^aElectrochemical Materials Science Division, Central Electrochemical Research Institute, Karaikudi 630 006, Tamilnadu, India

^bInstitute of Materials Research and Engineering, Singapore 117 602

Photoluminescence studies on pure and Eu³⁺-doped Sr₂CeO₄ compounds are presented. The pure compound displays a broad band in its emission spectrum when excited with 254 nm, which peaks at 467 nm and is due to the energy transfer between the molecular orbital of the ligand and charge transfer state of the Ce⁴⁺ ion. The excitation spectrum shows a broad band which peaks at 300 nm. From the spectral properties, it is established that Sr₂CeO₄ has good potential for application as a blue phosphor in low pressure mercury vapor lamps and in TV tubes. The Eu³⁺ spectral features, when doped at the Ce⁴⁺ site either singly or along with La³⁺, have been studied and compared with the results obtained by doping the Eu³⁺ ion at the Sr²⁺ site. At low Eu³⁺ concentrations (≤4 mol %), the observed excitation and emission spectra reveal excellent energy transfer between Ce⁴⁺ and Eu³⁺. This energy transfer generates white light with a color tuning from blue-white to red-white, the tuning being dependent on the Eu³⁺ concentration. At high Eu³⁺ concentrations (5-15 mol %), these compounds exhibit efficient red emission under 254, 355, and 466 nm excitations. The observed luminescence properties of these compounds are similar to those of the known Y₂O₃:Eu³⁺ red phosphor. The emission intensity of Sr₂CeO₄:Eu (>0.05) under 466 nm excitation is twice that of Y₂O₃:Eu. The results establish that the compound Sr₂CeO₄ is an efficient "single host lattice" for the generation of white and red lights under UV irradiation. © 2000 The Electrochemical Society. S0013-4651(99)08-024-4. All rights reserved.

Manuscript submitted August 9, 1999; revised manuscript received March 17, 2000.

Using novel combinatorial techniques, Danielson *et al.*¹ recently invented blue luminescence in the relatively simple mixed oxide of the formula Sr₂CeO₄ in the SrO-CeO₂ system. Under excitation by UV light ($\lambda_{\text{exc}} = 254$ nm), this compound exhibits photoluminescence due to the charge transfer mechanism, but this is not seen in SrCeO₃ or in any other Ce⁴⁺ containing oxidic compound with octahedral coordination. In addition, Sr₂CeO₄ was found to exhibit efficient luminescence under excitation with cathode and X-rays. Strangely, it was noted that the Ca- and Ba- analogues are not photoresponsive. Structural studies¹ have shown that Sr₂CeO₄ (crystal structure: orthorhombic; space group *Pbam*) consists of linear 1D chains of edge-sharing CeO₆ octahedra (which run parallel to the [001] crystallographic direction with repeat distance of 3.6 Å) with four equatorial μ^2 -O type atoms and two terminal Ce-O bonds per octahedron, surrounded by interchain Sr²⁺ cations. The terminal Ce-O bond lengths are slightly shorter than the equatorial Ce-O bond lengths indicating a slightly compressed CeO₆ octahedron and thus, lack of centrosymmetry. Detailed luminescence studies^{1,2} have established that Sr₂CeO₄ is a novel and a new host lattice for further studies as an efficient blue-white phosphor material.

It is well known from the studies on the commercial calcium halophosphate phosphor (CHP = Ca₅(PO₄)₃(F, Cl):Sb³⁺, Mn²⁺) that the mixing of blue light (~475 nm, Sb³⁺ emission) and orange light (~570 nm, Mn²⁺ emission) in proper ratio (Sb/Mn ratio) generates white light in this system under excitation by UV radiation of $\lambda = 254$ nm in the low pressure mercury vapor (lpmv) lamps.³⁻⁸ Similarly, the mixing of blue (450 nm, Eu²⁺ emission in Ba-Al-Mg-O or Sr-Al-O system), green (540 nm, Tb³⁺ emission in Ce-Tb-Mg-Al-O or Ce-Gd-Tb-Mg-B-O or La-Ce-Tb-P-O system) and red (610 nm, Eu³⁺ emission in Y₂O₃) colors in suitable proportion leads to white light emission in the rare earth based trichromatic phosphor blend (the so-called Color 80 or 90 lamps).⁸

Hence, by proper choice of the dopant ions, required emission colors can be arrived at, which when mixed suitably, would generate white light. However, the tricolor lamps contain different types of "host lattices", viz., complex aluminates, phosphates, and borates with different crystal structures and morphologies, and hence, pose problems for the manufacture of blends suitable for coating inside lpmv lamps. In other words, a single host lattice (similar to CHP),

when doped with various rare earth (Ln) ions either singly or in combination, which can generate white light in the lpmv is highly desirable. Efforts are being made world wide in the search for new and novel host lattices to act as single host phosphor.

Recently, we have studied in detail the luminescence properties^{9,10} of complex borates of the type Sr₆(MM')(BO₃)₆ (M, M' = metal ions including Ln), originally discovered by Keszlér and co-workers,¹¹ and established that they can act as excellent host lattices for the emission of red, green, and blue light upon UV irradiation. In view of the discovery of luminescence in Sr₂CeO₄, we thought it interesting to examine the effect of doping with europium on its light emitting properties. Our results show that indeed white light generation is possible by doping with small amounts of Eu. At higher dopant concentrations, red luminescence occurs and in addition, efficient energy transfer takes place between Ce⁴⁺ and Eu³⁺ energy levels. Herein we report the synthesis, characterization, and luminescence of pure and doped (at Sr- and Ce- sites) Sr₂CeO₄. The application potential of these compounds are highlighted by suitable comparison with standard commercial phosphors.

Experimental

The samples in polycrystalline form were synthesized by the conventional high temperature solid state reaction. The starting materials were: SrCO₃ (of 99.5% purity, Lumichem Ltd.), La₂O₃, Eu₂O₃, and CeO₂ (all of 99.99% purity, Indian Rare Earths Ltd.). La₂O₃ was heated in air at 1000°C for 24 h to remove moisture and CO₂ present in it and was kept in a desiccator. The starting materials taken in stoichiometric proportions were thoroughly homogenized in an agate mortar for 45 min and then transferred to alumina crucibles for heat treatment in air in a muffle furnace. The compounds were subjected to heat treatment at 1050-1150°C for 45-60 h with three intermediate grindings and heatings, and finally cooled to room temperature by furnace shut off. Powder X-ray diffractograms (XRDs) of the compounds were recorded using an automated Philips X-ray diffractometer (PW1820 generator; PW 1830 goniometer; Cu target attached with autodivergence receiving scattering slits; graphite monochromator; scintillation detector; PW1710 diffractometer control). The observed (*hkl*) reflections and their intensities were compared with the calculated ones generated using the computer program LAZY PULVERIX. The crystal data and the atom positions were taken from Danielson *et al.*¹ The lattice parameters were calculated from the indexed XRD patterns using least-squares refine-

* Electrochemical Society Active Member.

^z E-mail: gv-sr@imre.org.sg

ment. Powder density measurements were taken using pycnometric technique with xylene as the displacement liquid (a 5 mL specific gravity bottle and about 0.5 g of the sample). The thermal analysis measurements, thermogravimetric/differential thermal analysis, (TG/DTA) were carried out (range 25-1000°C, 10°C/min) using an automated system (STA 1500; PL Thermal Sci. Ltd., U.K.). Particle size analysis was carried out using a MALVERN (U.K.) particle sizer, type 3600E. The scanning electron micrographs (SEMs) of the samples were obtained using a Leica Stereoscan 440 model fitted with an E5000 Polaron coating unit (rating: 10 kV, 25 pA beam current). The samples for SEM studies were coated with a layer of gold to prevent charging of the specimen. The photoluminescence excitation and emission spectra were recorded at room temperature using a Hitachi 650-10S fluorescence spectrophotometer equipped with a 150 W xenon lamp and a Hamamatsu R928F photomultiplier detector. The spectra have been corrected for sample thickness and spurious effects. The reflectance of the samples were recorded at 254 nm by keeping both the excitation and emission slits at 254 nm and by measuring the intensity. A polished Al₂O₃ pellet was taken as the reference. The luminescence intensity measurements were carried out for samples taken in equal amounts and prepared under identical conditions. The standard phosphors Ca₅(PO₄)₃:Sb³⁺, ZnS:Ag⁺, and Y₂O₃:Eu³⁺ used for comparison purposes were synthesized in the laboratory.

Results and Discussion

Several samples of pure Sr₂CeO₄ and doped phases, Sr_{2-x}Eu_xCeO₄ and (Sr_{2-x}La_x)(Ce_{1-x}Eu_x)O₄ ($x = 0.0005-0.15$) in steps, have been synthesized by the solid-state reaction. Duplicate compositions have also been made to check on the consistency of behavior. The compounds are crystalline, very pale yellow in color, stable in air, and insoluble in water. The XRD patterns establish the single phase nature of the synthesized compounds and no second phase was noted. The least-squares fit orthorhombic lattice parameters for Sr₂CeO₄ are $a = 6.12$ Å; $b = 10.36$ Å, and $c = 3.59$ Å. These are in good agreement with the values $a = 6.119$ Å; $b = 10.349$ Å; and $c = 3.597$ Å reported by Danielson *et al.*¹ The powder density of the compound Sr₂CeO₄ (measured: 5.37; theoretical 5.52 g/cm³) obtained by the pycnometric techniques is found to be >97% of the theoretical value. The TG/DTA carried out in air on the synthesized compound Sr₂CeO₄ indicates no phase transition or weight loss in the range 25-1000°C. Particle size analysis showed that the particle sizes are in the range 7-27 μm. The SEM studies revealed the polycrystalline nature of Sr₂CeO₄ consisting of particles irregular in shape and size. While at low magnification the particles appear agglomerated, at high enough magnification, the nature of the individual crystallites (dense and without any voids) is clearly evident (Fig. 1).

Sr₂CeO₄: A New Blue Phosphor

The excitation spectrum recorded for the compound Sr₂CeO₄ at room temperature displays a broad band with two peaks, one in the range 297-305 nm and the other at around 342-350 nm (broad shoulder), as shown in Fig. 2a. This band could be assigned to the transition $t_{1g} \rightarrow f$, where f is the lowest excited charge transfer state of the Ce⁴⁺ ion and t_{1g} is the molecular orbital of the surrounding ligand in sixfold oxygen coordination.^{1,12} This broad band is the charge transfer (CT) band of the Ce⁴⁺ ion and extends from 220-400 nm. Hence, it is possible to excite the Ce⁴⁺ ion in this lattice with 254 nm. Hence, it is possible to excite the Ce⁴⁺ ion in this lattice with 254 nm to check for its suitability for application in lpmv lamps. In addition, efficient excitation with radiation of wavelengths in the range 354-365 nm is also possible, which is compatible with cathode ray excitation.

When excited with the radiation of wavelength 254 nm, Sr₂CeO₄ emits a broad band in the blue region which extends from 380-600 nm with a peak around 460-480 nm (Fig. 2b). This is in agreement with the results of Danielson *et al.*¹, and the band can be assigned to the $f \rightarrow t_{1g}$ transition of Ce⁴⁺. The luminescence¹ and reflectivity properties as shown in Table I, are comparable with those exhibited by known standard phosphors when excited with $\lambda = 254$ nm though the measured quantum efficiency is <50%. The emission spectrum of Sr₂CeO₄ observed with 355 nm excitation is similar to

that observed with 254 nm excitation; the only difference is the appearance of a weak band at 404 nm in addition to the broad band, on excitation with 355 nm (Fig. 2b). The value of integrated emission intensity for excitation with 355 nm is higher than that for excitation with 254 nm (Table I). The emission spectrum observed for excitation with 300 nm looks similar to the one observed under 355 nm, the integrated emission intensity being high in the former case. Since our interest is to check the emission features under 254 nm excitation only, we did not carry out detailed studies on the excitation with 300 nm.

Sr₂CeO₄:Eu

White Light Generation in Single Host at Low Eu³⁺ Concentration

Sr₂CeO₄:Eu, La system.—In order to study the Eu³⁺ luminescence features and the possible energy migration between Ce⁴⁺ and Eu³⁺ to generate white light, compounds of the nominal compositions (Sr_{2-x}La_x)(Ce_{1-x}Eu_x)O₄ (hereafter referred to as A) where $x = 0.001-0.05$ have been synthesized and subjected to photoluminescence studies. Since the stable valency of Eu is trivalent (3+) and is doped at the 6-(hexa) coordinated tetravalent (4+) Ce site, the La³⁺ is doped at the Sr²⁺ (divalent) site for the charge balance. The ionic radii of the ions permit this incorporation ($r_{Ce^{4+}} = 0.87$ Å; $r_{Eu^{3+}} = 0.95$ Å).¹³ It must be mentioned, however, that the nominal compositions may not represent the unique charge compensation mechanism mentioned above, and several other defect structure models are possible and should be taken in to account to describe the possible environment of the Eu ions in the Sr₂CeO₄ lattice. The excitation spectrum recorded for A with $x = 0.001$ for $\lambda_{em} = 467$ nm (not shown in Fig. 3) shows a broad band with two peaks, one at ~300-305 nm and the other at ~344-350 nm, which is similar to the exci-

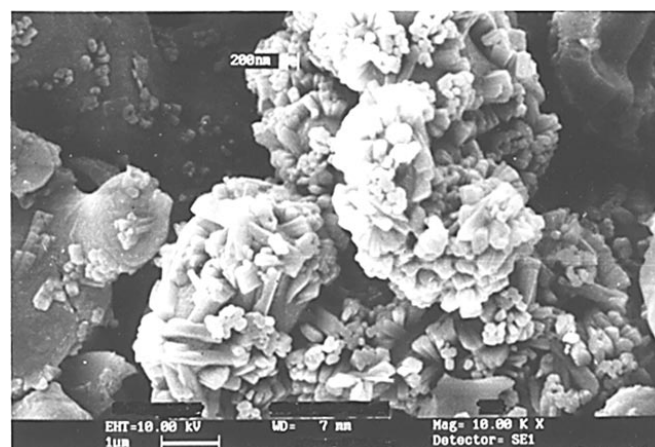
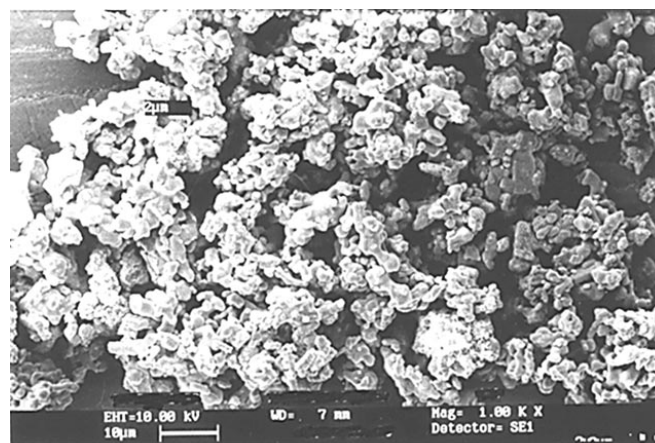


Figure 1. SEM photographs of Sr₂CeO₄ at two different magnifications.

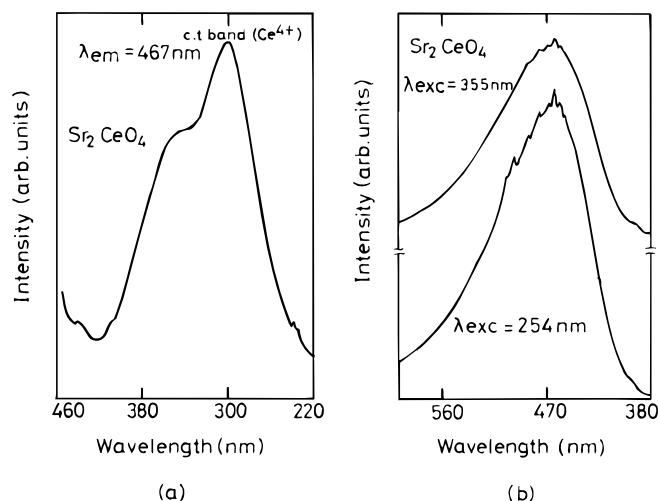


Figure 2. (a) Excitation and (b) emission spectra of pure Sr_2CeO_4 . Excitation and emission wavelengths are given.

tation spectrum of the undoped Sr_2CeO_4 . This band is due to the $\text{Ce}^{4+}\text{-O}^{2-}$ CT and the peak at ~ 300 nm is of high intensity. The excitation spectrum recorded for the above composition ($\lambda_{\text{em}} = 614$ nm, Eu^{3+} emission) (Fig. 3a) shows the above CT band and the Eu^{3+} excitation lines at 397 nm (${}^7\text{F}_0 - {}^5\text{L}_6$), 466 nm (${}^7\text{F}_0 - {}^5\text{D}_2$), and 536 nm (${}^7\text{F}_0 - {}^5\text{D}_1$) (of which the intensity of the 466 nm line is the highest). At low concentration ($x = 0.001$) of Eu^{3+} , the intensities of the Eu^{3+} excitation lines are very weak when compared with that of the CT band of Ce^{4+} . As is well known, in the case of hexa-coordination, the charge transfer band of Eu^{3+} lies in the high energy region and is not host lattice dependent.^{4,14} Therefore, it is highly probable that in Sr_2CeO_4 the CT band of Eu^{3+} lies in the high energy region. Since the molar absorption coefficient of Ce^{4+} is very high when compared with that of Eu^{3+} and since Eu^{3+} is substituted at the Ce^{4+} site, it is possible that the CT band of Ce^{4+} inhibits the CT band of Eu^{3+} in this lattice. As the concentration of Eu^{3+} is increased, we observed that the intensity of the $\text{Ce}^{4+}\text{-O}^{2-}$ CT band gets diminished while the intensities of the Eu^{3+} excitation lines (mainly the intensity of line at 466 nm) start increasing. This clearly indicates the energy migration between the ions Ce^{4+} and Eu^{3+} in Sr_2CeO_4 as the concentration of the Eu^{3+} ion increases (0.01-0.05) (Fig. 3b-d).

The emission spectrum recorded for A (with $x = 0.001$), when excited with radiation of wavelength 254 nm (as well as with 355 nm), displays a broad band which peaks at $\sim 460\text{-}480$ nm (Fig. 4a). This broad band is due to the $f \rightarrow t_{1g}$ transition of Ce^{4+} in the compound Sr_2CeO_4 and it covers all the Eu^{3+} emission lines up to 650 nm. The

Eu^{3+} emission lines appear as weak shoulders in the Ce^{4+} emission band. When the Eu^{3+} concentration is increased to 0.005 mol, the intensities of the Eu^{3+} emission lines (mainly ${}^5\text{D}_0 - {}^7\text{F}_1$ at 582 nm and ${}^5\text{D}_0 - {}^7\text{F}_2$ at 614 nm) start increasing (Fig. 4b). The intensities of both the above transitions are almost equal (ratio ~ 1) and is almost constant in the Eu concentration range $x = 0.001\text{-}0.05$. The intensities of the ${}^5\text{D}_0 - {}^7\text{F}_{1,2}$ transition lines show a low value when compared with the intensity of the Ce^{4+} emission band for $x = 0.005$. The ${}^5\text{D}_0 - {}^7\text{F}_{1,3,4}$ transition lines are also very weak in intensity. The ${}^5\text{D}_0 - {}^7\text{F}_0$ transition is present at 578 nm and is a single peak which shows that there is only one site for Eu^{3+} in this lattice.⁴ Even though lines in the blue and the green regions are present, they are very weak in intensity. For A with $x = 0.02$, the emission intensities of the Eu^{3+} lines are found to be high, when compared with those of the Ce^{4+} emission band (Fig. 4d). At this concentration and above, the intensity of the Ce^{4+} emission band is found to be reduced gradually. Also, the intensities of the Eu^{3+} lines in the blue and green regions start increasing for $x = 0.02\text{-}0.05$ for A. This reveals an excellent energy transfer from Ce^{4+} to Eu^{3+} in Sr_2CeO_4 . When seen under UV light of wavelength 254 (or 355 nm), the $(\text{Sr}_{2-x}\text{La}_x)(\text{Ce}_{1-x}\text{Eu}_x)\text{O}_4$ compounds display colors ranging from blue-white to red-white within the concentration range $x = 0.001\text{-}0.05$.

$\text{Sr}_2(\text{Ce}, \text{Eu})\text{O}_4$ system.—It is well known that the net effective charge of the crystal lattice plays a major role on the luminescence efficiency of the dopant ion in the lattice under CT excitation.¹⁵ If the net charge is negative, the efficiency will increase in the case of lanthanide ions.¹⁶ In the case of Sr_2CeO_4 , the CT band of Ce^{4+} dominates due to its high value of absorption. It is observed that the CT bands of Ce^{4+} and Eu^{3+} are found to resemble each other in character.^{12,14} Therefore, explanations based on the configuration coordinate model discussed by vander Voort and Blasse¹⁵ for Eu^{3+} could also be applied to Ce^{4+} . To investigate the influence of the net charge on the luminescence efficiency of the dopant ion (here Eu^{3+}) as well as to study the possible luminescence features, we have synthesized and studied the compounds of the nominal composition, $\text{Sr}_2\text{Ce}_{1-x}\text{Eu}_x\text{O}_4$ (hereafter referred to as B) where $x = 0.0005\text{-}0.05$. Here, since the trivalent Eu ion replaces the Ce^{4+} ion and there is no cation charge compensator, oxygen vacancies must exist or the net charge is negative. The excitation spectrum recorded for B with $x = 0.0005$ ($\lambda_{\text{em}} = 467$ nm) shows a broad band (the Ce^{4+} CT band) with two peaks, one at ~ 310 nm and the other at ~ 350 nm, of which the peak at 350 nm is intense. As the concentration of the Eu^{3+} ion is increased, the intensity of the peak at ~ 350 nm starts decreasing while that of the peak at ~ 310 nm starts increasing up to the value $x < 0.02$ of Eu. For $x = 0.02\text{-}0.04$, the peak at 310 nm dominates in intensity.

The excitation spectrum recorded for B with $x = 0.0005$, by keeping the emission wavelength at 614 nm (Eu^{3+} lines) shows the intense Ce^{4+} emission band and the weak Eu^{3+} lines, similar to the

Table I. Comparison of the luminescence properties of Sr_2CeO_4 and the standard blue phosphors.

Property	Sr_2CeO_4	$\text{Ca}_5(\text{PO}_4)_3\text{F}:\text{Sb}^{3+}$	$\text{ZnS}:\text{Ag}^+$
Color (in white light)	Very pale-yellow	White	White (gray-white)
Crystal system	Orthorhombic	Hexagonal	Face centered cube
Coordination of the luminescent center	Six (Ce^{4+})	Nine (Sb^{3+})	(Zn^{2+}) ^a
Color of emission, λ_{max}	Broad band-blue region (467 nm)	Broad band-blue region (475 nm)	Broad band-blue region (450 nm)
Integrated emission intensity (254 nm excitation) (counts)	64	100	18
Integrated emission intensity (355 nm excitation) (counts)	81	—	100
Reflectance at 254 nm ^b	8	12	12

^a It is the bandgap and not the luminescent center which decides the emission in ZnS. Given here for comparison.

^b Value measured for the polished Al_2O_3 pellet is taken as 100 (in counts).

situation in A. Increase in Eu^{3+} concentration ($x = 0.01$ - 0.02) increases the intensities of the Eu^{3+} lines and the line at 466 nm is dominant as shown in Fig. 5a.

The emission spectrum of B with $x = 0.0005$ under 254 nm excitation shows the Ce^{4+} emission band (peak ~ 467 nm) which covers all the Eu^{3+} lines (weak shoulders) up to 650 nm. This happens up to a Eu concentration of $x = 0.01$, and for higher x , the Eu^{3+} emission lines dominate in intensity (Fig. 5b). Unlike the previous case (A), in this compound (B) the Eu^{3+} emission lines at 614 nm (${}^5\text{D}_0 - {}^7\text{F}_2$) is more intense than the Eu^{3+} line at 583 nm (${}^5\text{D}_0 - {}^7\text{F}_1$). The ratio of the intensities is >1 . This may be due to the stiff surroundings (octahedral coordination) of the Eu^{3+} ion. We found that the line due to ${}^5\text{D}_0 - {}^5\text{F}_0$ transition cannot be clearly observed under 254 nm excitation, but could be seen at 578 nm when excited with 466 nm.

(*Sr, Eu*) $_2\text{CeO}_4$ system.—In this case, the Eu^{3+} is doped at the Sr^{2+} site and hence, either Sr vacancies exist in the lattice or the net

charge is positive. To study the luminescence properties, compounds with nominal composition, $\text{Sr}_{2-x}\text{Eu}_x\text{CeO}_4$ (hereafter referred to as C) with $x = 0.04$ - 0.10 , have been synthesized. For a composition of C with $x = 0.04$, the recorded emission spectrum ($\lambda_{\text{exc}} = 254$ nm) shows a dominant Eu^{3+} line at 614 nm and a weak Ce^{4+} emission band. The intensity of the ${}^5\text{D}_0 - {}^7\text{F}_2$ transition line (614 nm) is very

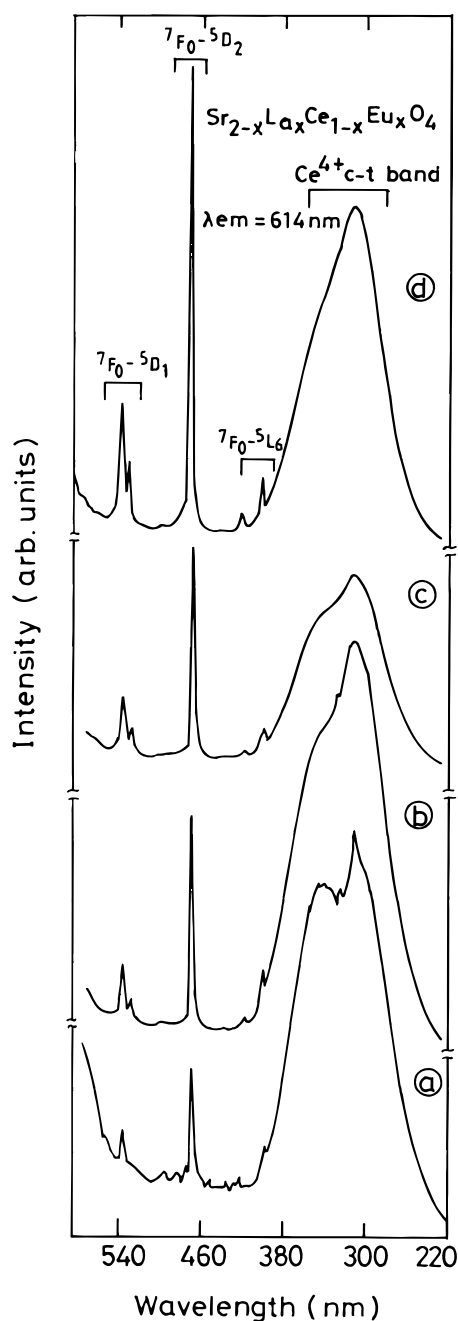


Figure 3. Excitation spectra of $\text{Sr}_{2-x}\text{La}_x\text{Ce}_{1-x}\text{Eu}_x\text{O}_4$ for different x values. (a) $x = 0.001$, (b) $x = 0.005$, (c) $x = 0.01$, (d) $x = 0.02$, (e) $x = 0.05$.

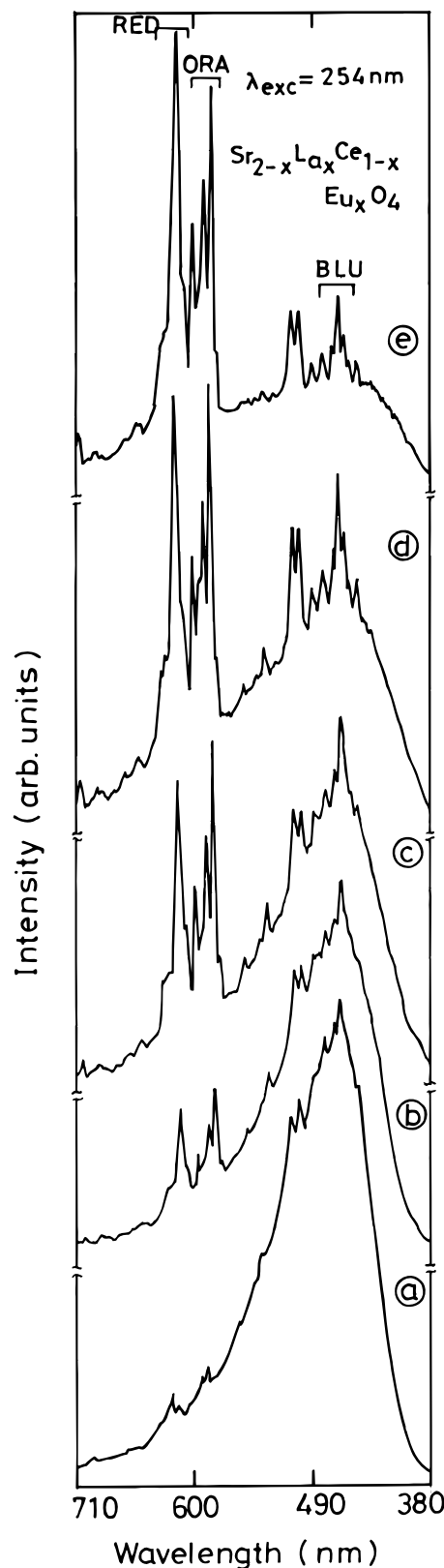


Figure 4. Emission spectra of $\text{Sr}_{2-x}\text{La}_x\text{Ce}_{1-x}\text{Eu}_x\text{O}_4$ for different x values. (a) $x = 0.001$, (b) $x = 0.005$, (c) $x = 0.01$, (d) $x = 0.02$, (e) $x = 0.05$. RED denotes red emission due to ${}^5\text{D}_0 - {}^7\text{F}_2$ transition of Eu^{3+} , ORA denotes orange emission due to ${}^5\text{D}_0 - {}^7\text{F}_1$ transition of Eu^{3+} , and BLU denotes blue emission due to $f \rightarrow t_{1g}$ transition of Ce^{4+} , in this figure and in the subsequent figures.

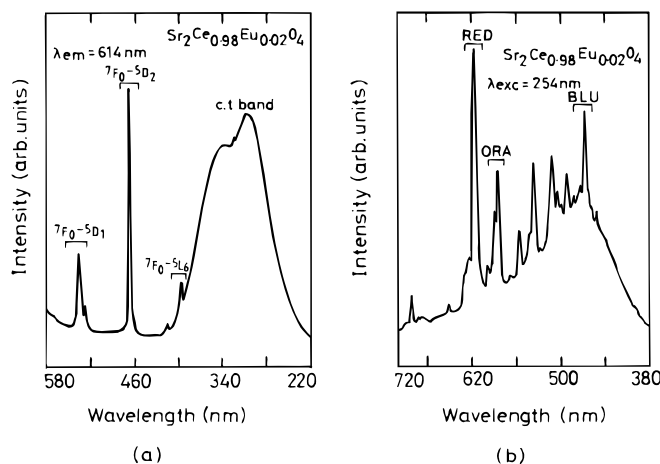


Figure 5. (a) Excitation and (b) emission spectra of $\text{Sr}_2\text{Ce}_{0.98}\text{Eu}_{0.02}\text{O}_4$.

high when compared with that of the $^5\text{D}_0 - ^7\text{F}_1$ transition (583 nm). The presence of intense $^5\text{D}_0 - ^7\text{F}_2$ transitions in the compounds A, B, and C confirms the presence of a noncentrosymmetric site for Eu^{3+} in Sr_2CeO_4 . The $^5\text{D}_0 - ^7\text{F}_0$ transition line is clearly observable at 578 nm when excited with 466 nm, as is the case of the compound B. The excitation spectra observed for different emission wavelengths ($\lambda_{\text{em}} = 467$ and 614 nm) show the CT band of Ce^{4+} (with the peak at ~ 308 nm as dominant) and the Eu^{3+} excitation lines. However, the intensities of the Eu^{3+} excitation lines are more when compared with those of the CT band of Ce^{4+} . Neither the net positive charge nor the larger ionic size of Sr^{2+} seems to reduce the intensity of the line due to Eu^{3+} ion, when compared with the situations encountered in compounds A and B.

Depending on the Eu^{3+} concentration, the compounds A, B, and C all display emission colors ranging from blue-white to red-white, when seen under UV light of $\lambda = 254$ and 355 nm. Hence, this offers the possibilities of generating white light in Sr_2CeO_4 under lpmv and cathode ray excitations. It is observed that similar to the known CHP and the trichromatic lamp phosphors (TLPs), the compound $\text{Sr}_2\text{CeO}_4:\text{Eu}$ also emits in the region of visible light covering violet-blue to red. For values of x in the range 0.005-0.015, the compound $\text{Sr}_2\text{CeO}_4:\text{Eu}$ gives white light emission under 254 and 355 nm excitation when seen with the naked eye, similar to CHP and TLP. However, optimization of the Eu concentration, particle size and morphology, addition of other complementary compounds (both blank and luminescent) need to be done for this Sr_2CeO_4 single host lattice to yield white light emission matching in color (both color coordinates and color rendering index) with the known CHP and TLP (Color 80 or 90).

$\text{Sr}_2\text{CeO}_4:\text{Eu}$

A Potential Red Phosphor at High Eu Concentrations

The above results show that irrespective of the site(s) at which Eu^{3+} is doped in Sr_2CeO_4 , the red emission at 614 nm dominates

under excitation with 254 (and 466 nm) as the Eu^{3+} concentration (x) is increased to 0.05 and above. This suggests that $\text{Sr}_2\text{CeO}_4:\text{Eu}$ (0.05-0.15) has ample potential for application as a red phosphor in lpmv lamps, similar to the well-known $\text{Y}_2\text{O}_3:\text{Eu}^{3+}$ red phosphor. The observed emission spectrum shows that in the case of A, both orange ($^3\text{D}_0 - ^7\text{F}_1$) and red ($^5\text{D}_0 - ^7\text{F}_2$) color emissions dominate, the latter with higher intensity when excited with 254 nm. In the case of B and C, we observed that only the red emission line at 614 nm dominates in intensity. The integrated emission intensities of all these compounds along with $\text{Y}_2\text{O}_3:\text{Eu}$ are given in Table II. From the observed spectra (Fig. 6), it could be concluded that the compounds B and C are potential candidates for application in lpmv lamps as red phosphors. But the host lattice must be suitably modified to achieve emission intensities equal to or greater than the known $\text{Y}_2\text{O}_3:\text{Eu}^{3+}$ phosphor under 254 nm. We found that the compounds A, B, and C also show sufficiently high intensity under excitation with long wavelength UV and hence could also be attempted for application as a red phosphor in high pressure mercury vapor (hpmv) lamps and perhaps in TV tubes.

When excited with the dominant 466 nm, we observed that in the compounds A, B, and C, the intensity of the $^5\text{D}_0 - ^7\text{F}_2$ (614 nm) transition is higher than the intensity observed under excitation with 254 nm. The observed luminescence spectral features (under 466 nm excitation) appear similar to each other and also similar to those observed in the $\text{Y}_2\text{O}_3:\text{Eu}^{3+}$ red phosphor. But the intensities are twofold higher than the intensity of $\text{Y}_2\text{O}_3:\text{Eu}^{3+}$, indicating the excellent application potential of $\text{Sr}_2\text{CeO}_4:\text{Eu}$ under this excitation (Table II and Fig. 7). If properly pumped in the blue region, this compound could be utilized for application in lasers as a red laser material pumped in the blue region.¹⁷ The only dominant emission line is the line due to the $^5\text{D}_0 - ^7\text{F}_2$ transition at 614 nm. All the other lines are very weak in intensity and therefore, there is no probability for the presence of the orange and green Eu^{3+} emission lines (Fig. 7). The excitation spectra obtained for A, B, and C ($\lambda_{\text{em}} = 614$ nm) show a Ce^{4+} (Eu^{3+}) CT band with a single peak at ~ 306 nm. The line at 466 nm due to $^7\text{F}_0 - ^5\text{D}_1$ transition is of high intensity. At both low and high Eu^{3+} concentrations, the dominant levels ($^5\text{D}_0 - ^7\text{F}_{1,2}$) show splitting due to the crystalline electric field (CEF) effects.

Energy Transfer Mechanism in $\text{Sr}_2\text{CeO}_4:\text{Eu}^{3+}$

In luminescent materials, energy transfer mechanisms between ions of the same or different types and between the host and the activator are well known.^{4,5,7,8,18} They are either due to resonance or exchange interactions or multipolar interactions between the ions of the same or different types and depend on the critical energy transfer distance (R_c) between the absorbing groups in the crystal lattice.^{4,5} In addition, the lifetime of the excited state of the sensitizer ion also plays a major role, and both radiative and nonradiative processes of energy transfer can occur.

In the excitation spectra of Eu^{3+} ($\lambda_{\text{em}} = 614$ nm) in Sr_2CeO_4 we observed that at low Eu concentrations, the Ce^{4+} emission band is present. When excited under CT excitation wavelength, the Ce^{4+} emission band is observed together with the Eu excitation lines. The Ce^{4+} emission band is found to cover all the Eu excitation lines up to 540 nm (mainly the dominant 466 nm) indicating that Ce transfers

Table II. Comparison of the luminescence properties of $\text{Sr}_2\text{CeO}_4:\text{Eu}$ and the standard red phosphor $\text{Y}_2\text{O}_3:\text{Eu}$.

Phosphor	Integrated emission intensity		Reflectance at 254 nm ^a (counts)
	$\lambda_{\text{exc}} = 254$ nm (counts)	$\lambda_{\text{exc}} = 466$ nm (counts)	
$\text{Sr}_{2-x}\text{La}_x\text{Ce}_{1-x}\text{Eu}_x\text{O}_4$ ($x = 0.08$)	31	84	5
$\text{Sr}_2\text{Ce}_{1-x}\text{Eu}_x\text{O}_4$ ($x = 0.08$)	44	100	6
$\text{Sr}_{2-x}\text{Eu}_x\text{CeO}_4$ ($x = 0.08$)	44	87	5
$\text{Y}_{2-x}\text{Eu}_x\text{O}_3$ ($x = 0.06$)	100	49	16

^a Value measured for the polished Al_2O_3 pellet is taken as 100 (counts).

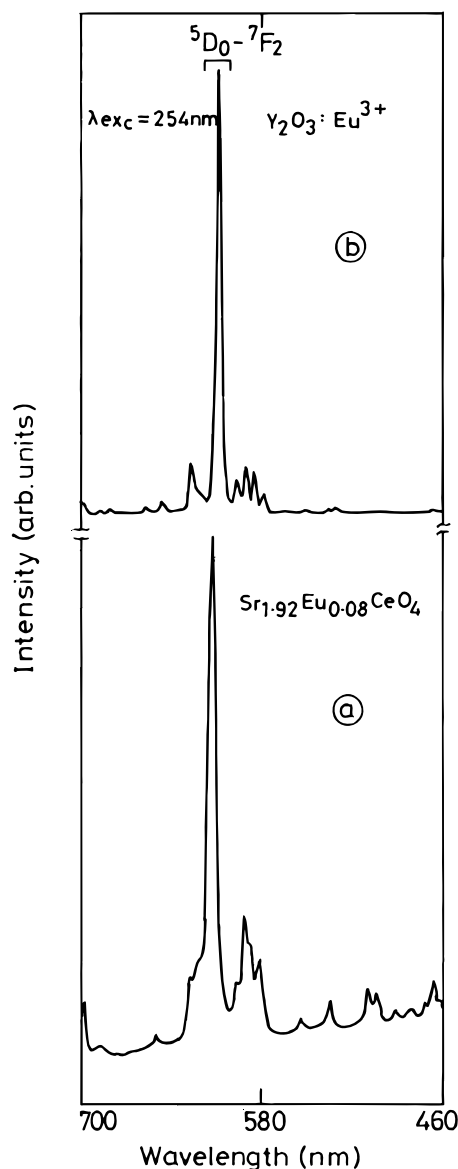


Figure 6. Emission spectra of (a) $\text{Sr}_{2-x}\text{Eu}_x\text{CeO}_4$ ($x = 0.08$) and (b) $\text{Y}_2\text{O}_3:\text{Eu}$ (3 mol %).

some of its energy to the Eu ion. Increase in Eu concentration increases the intensity of Eu lines with a corresponding decrease in the intensity of the Ce emission band. Thus, the energy transfer is incomplete and it is highly probable that both radiative and nonradiative energy transfers occur in $\text{Sr}_2\text{CeO}_4:\text{Eu}$ with Ce acting as the sensitizer and Eu ion as the activator in the host matrix.

At high Eu^{3+} concentrations ($x = 0.05$ - 0.15), the excitation spectra of Eu^{3+} (in the compounds A, B, and C) show the presence of both Ce^{4+} and Eu^{3+} excitation bands. But in the emission spectra under CT excitations, only the Eu^{3+} emission lines are observed and the Ce^{4+} ion emission is totally quenched. Thus, for $x > 0.05$, the energy transfer to the Eu^{3+} ion from the Ce^{4+} ion in Sr_2CeO_4 is complete and nonradiative. It is well known that the energy transfer from a broad band emitter to a line emitter is only possible for nearest neighbors in the lattice.⁴ In the compound Sr_2CeO_4 , the crystal structure is one-dimensional with a fairly short interchain distance of 3.597 \AA (c -lattice parameter). The lifetime of Ce^{4+} in the undoped Sr_2CeO_4 has been measured to be unusually long ($51 \mu\text{s}$).¹ Hence, there is a high probability of energy transfer due to exchange interactions [since $3.6 \text{ \AA} < R_c$ for exchange interaction (5 \AA)] which can occur between Ce^{4+} and Eu^{3+} ions in different chains in addition to that within the chains. But a reliable conclusion can be arrived at only after detailed investigations on well-defined single crystal samples.

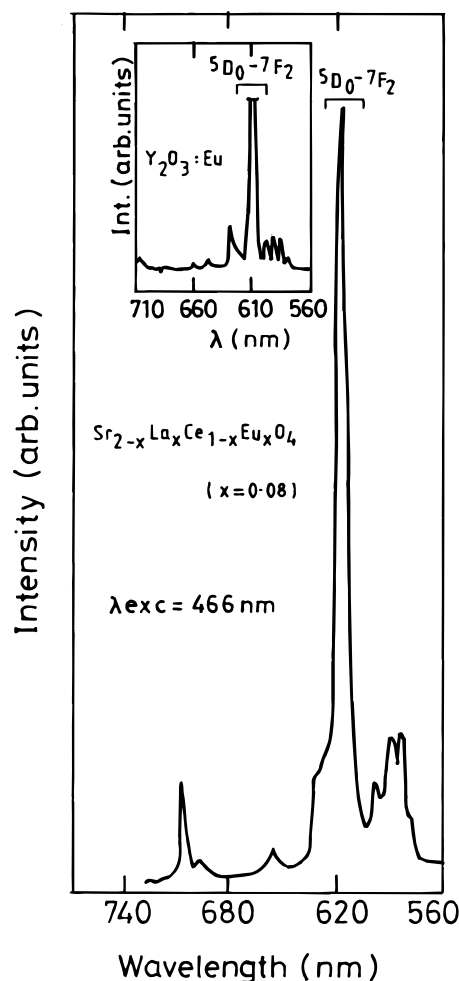


Figure 7. Emission spectra of $\text{Sr}_{2-x}\text{La}_x\text{Ce}_{1-x}\text{Eu}_x\text{O}_4$ ($x = 0.08$). Inset shows the emission spectrum of $\text{Y}_2\text{O}_3:\text{Eu}$ (3 mol %) for comparison.

Conclusions

Pure and the Eu^{3+} -doped Sr_2CeO_4 compounds have been synthesized by the high temperature solid state reaction and characterized by powder XRD, TG/DTA, density, particle size, and SEM studies. The luminescence properties of the undoped Sr_2CeO_4 blue phosphor have been compared with the known blue phosphors to highlight its application potential. The Eu^{3+} luminescence in Sr_2CeO_4 has been reported for the first time. The energy transfer between Ce^{4+} and Eu^{3+} occurs at low (and also at high) Eu concentrations and generation of white light is established under 254 and 355 nm excitation. Efficient red phosphors have been identified under different excitation wavelengths at high Eu^{3+} concentrations ($x \geq 0.08$) in $\text{Sr}_{2-x}\text{Eu}_x\text{CeO}_4$ and $(\text{SrLa})(\text{CeEu})\text{O}_4$ and have been compared with the standard phosphor. The salient features of the 1D crystal structure of Sr_2CeO_4 along with the unusually long excited state lifetime, easy synthesis, good possibilities of controlling the particle size and morphological features guarantee the potential of this host lattice for application as a phosphor under excitation with UV, cathode, and X-rays. Other dopant ions (rare earth and transition metal) are being tried and the results will be published elsewhere.

Acknowledgments

The authors thank Dr. R. Jagannathan for extending the phosphor laboratory facilities, R. Sakthivel (RRL, Bhubaneswar) for powder XRD, Dr. V. Sundaram for TG/DT, L. K. Srinivasan for particle size, Dr. S. R. Sainkar (NCL, Pune) for SEM studies, S. Angappan for computer help and S. P. Pandurangan for drawings. R.S. thanks the Council of Scientific & Industrial Research, Government of India, for financial assistance.

The Institute of Materials Research and Engineering assisted in meeting the publication costs of this article.

References

1. E. Danielson, M. Devenney, D. M. Giaquinta, J. H. Golden, R. C. Haushalter, E. W. Mc Farland, D. M. Poojary, C. M. Reaves, W. H. Weinberg, and X. D. Wu, *Science*, **279**, 837 (1998) (and supplementary data); *J. Mol. Struct.*, **470**, 229 (1998).
2. Y. D. Jiang, F. L. Zhang, C. J. Summers, and Z. L. Wang, *Appl. Phys. Lett.*, **74**, 1677 (1999).
3. K. H. Butler, *Fluorescent Lamp Phosphors*, The Pennsylvania State University Press, University Park, PA (1980).
4. G. Blasse and E. C. Grabmaier, *Luminescent Materials*, Springer-Verlag, Berlin (1994).
5. B. M. J. Smets, *Mater. Chem. Phys.*, **16**, 283 (1987).
6. G. V. Subba Rao, in *Perspectives in Solid State Chemistry*, K. J. Rao, Editor, p. 366, Narosa Publishers, Delhi, India (1995).
7. C. Fouassier, *Curr. Opin. Solid State Mater. Sci.*, **2**, 231 (1997).
8. C. R. Ronda, T. Justel, and H. Nikol, *J. Alloys Compd.*, **275-277**, 669 (1998); T. Justel, H. Nikol, and C. Ronda, *Angew. Chem. Int. Ed.*, **37**, 3084 (1998).
9. R. Sankar and G. V. Subba Rao, *J. Alloys Compd.*, **281**, 126 (1998).
10. G. V. Subba Rao and R. Sankar, Indian Pat. Application NF-333/9T; NF-107/98, 1997.
11. K. I. Schaffers, P. D. Thompson, T. Alekel III, J. R. Cox, and D. A. Keszler, *Chem. Mater.*, **6**, 2014 (1994).
12. H. E. Hoefdraad, *J. Inorg. Nucl. Chem.*, **37**, 1917 (1975).
13. R. D. Shannon, *Acta Crystallogr.*, **A32**, 751 (1976).
14. H. E. Hoefdraad, *J. Solid State Chem.*, **5**, 175 (1975).
15. D. vander Voort and G. Blasse, *J. Solid State Chem.*, **87**, 350 (1990); D. vander Voort and G. Blasse, *J. Phys. Chem. Solids*, **52**, 1149 (1991); D. vander Voort and G. Blasse, *Chem. Mater.*, **3**, 1041 (1991); D. vander Voort, J. M. E. de Rijk, R. van Doorn, and G. Blasse, *Mater. Chem. Phys.*, **31**, 333 (1992).
16. J. Alarcon, D. vander Voort, and G. Blasse, *Mater. Res. Bull.*, **27**, 467 (1992).
17. R. Jagannathan, *J. Lumin.*, **68**, 211 (1996).
18. L. E. Shea, R. K. Datta, and J. J. Brown, Jr., *J. Electrochem. Soc.*, **141**, 1950 (1994).